

Dielectric behavior of oblate spheroidal particles: Application to erythrocytes suspensions

J. P. Huang and K. W. Yu

Department of Physics, The Chinese University of Hong Kong, Shatin, NT, Hong Kong

Abstract

We have investigated the effect of particle shape on the electrorotation (ER) spectrum of living cells suspensions. In particular, we consider coated oblate spheroidal particles and present a theoretical study of ER based on the spectral representation theory. Analytic expressions for the characteristic frequency as well as the dispersion strength can be obtained, thus simplifying the fitting of experimental data on oblate spheroidal cells that abound in the literature. From the theoretical analysis, we find that the cell shape, coating as well as material parameters can change the ER spectrum. We demonstrate good agreement between our theoretical predictions and experimental data on human erythrocytes suspensions.

PACS Number(s): 82.70.-y, 87.22.Bt, 77.22.Gm, 77.84.Nh

I. INTRODUCTION

Dielectrophoresis and electrorotation (ER) offer a unique capability of monitoring the dielectric properties of dispersions of colloids and biological cells. Under the action of external fields, these particles exhibit rich fluid-dynamic behaviors as well as various dielectric responses. It is of importance to investigate their frequency-dependent responses to ac electric fields, which yields valuable information on the structural (Maxwell-Wagner) polarization effects [1,2]. The polarization is characterized by a variety of characteristic frequency-dependent changes known as the dielectric dispersion. In particular, for the β -dispersion (also called the Maxwell-Wagner dispersion, ranging from KHz to MHz), it may suffice to focus on the induced dipole moments of the particles. In this work, we will analyze the β -dispersion based on the spectral representation theory.

In the last two decades, various experimental tools have been developed to analyze the polarization of biological cells - dielectric spectroscopy [3], dielectrophoresis [4] and ER [5] techniques. Among these techniques, conventional dielectrophoresis and ER are usually applied to analyze the frequency dependence of translations and rotations of individual cells in an inhomogeneous and rotating electric field, respectively [4,5]. Moreover, one is able to monitor the cell movements by using automated video analysis [6] as well as light scattering methods [2]. As a matter of fact, the general cause of ER is the existence of a phase difference between the field-induced dipole moment and the external rotating field, resulting in a desired torque which causes the cells to rotate.

In the dilute limit, the ER of individual cell can be predicted by ignoring the mutual interaction between the cells. However, the cells may aggregate under the influence of the external field. In this case the Brownian motion can be neglected, and the cell system becomes non-dilute even though it is initially dilute. As an initial model, we have recently studied the ER of two approaching spherical particles in the presence of a rotating electric field [7]. We showed that when the two particles approach and finally touch, the mutual polarization interaction between the particles leads to a change in the dipole moment of

individual particles and hence the ER spectrum, as compared to that of isolated particles, via the multiple image method [8].

In this work, we consider further the effects of cell shape on the ER spectrum. In fact, a cell may readily deviate from a perfect spherical shape due to many reasons, e.g., under a hydrostatic pressure [9]. In addition to a prolate spheroidal shape [10], there exist cells of oblate spheroidal shape, such as human erythrocytes.

Regarding the spectral representation approach [11], it is a rigorous mathematical formalism of the effective dielectric constant of a two-phase composite material. Also, the approach was extended to deal with a three-phase material [12]. The spectral approach offers the advantage of the separation of material parameters (namely the dielectric constant and conductivity) from the cell structure information, thus simplifying the study. From this approach, one can readily derive the dielectric dispersion spectrum, with the dispersion strength as well as the characteristic frequency being explicitly expressed in terms of the structure parameters and the materials parameters of the cell suspension [13]. In the present work, the analytic expression for the characteristic frequency is derived with the aid of the spectral representation approach, thus simplifying the fitting of experimental data. We show good agreement with experimental data on human erythrocytes [14].

II. FORMALISM

Consider a suspension of spheroidal particles of complex dielectric constant $\tilde{\epsilon}_1$ coated with a shell of $\tilde{\epsilon}_s$ dispersed in a host medium of $\tilde{\epsilon}_2$, where

$$\tilde{\epsilon} = \epsilon + \sigma/i2\pi f \quad (1)$$

with f being the frequency of the applied field $\mathbf{E}_0 = E_0\hat{\mathbf{z}}$. The depolarization factors of the spheroidal particles is described by a sum rule

$$L_z + 2L_{xy} = 1 \quad (2)$$

where $L_z(1/3 < L_z < 1)$ and $L_{xy}(= L_x = L_y)$ are the depolarization factors along the z - and x - (or y -) axes of the oblate spheroidal particle, respectively. $L_z = L_{xy} = 1/3$ just indicates sphere, while $L_z = 1$ disk.

The phenomenon of ER is based on the interaction between a rotating electric field \mathbf{E} and the induced dipole moment \mathbf{M} . The dipole moment of the particle arises from the induced charges that accumulate at the interface of the particle. In circularly polarized fields, the axis of lowest polarizability, namely z -axis of the present particle, should be oriented perpendicular to the plane of field rotation [15].

The angle between \mathbf{M} and \mathbf{E} is denoted by θ , where $\theta = \omega \times \text{time}$ and $\omega = 2\pi f$ is angular velocity of the rotating electric field. The torque acting on the particle is given by the vector cross product between the electric field and the dipole moment, so that only the imaginary part of the dipole moment contributes to the ER response. In the steady state, the frequency-dependent rotation speed $\Omega(f)$, which results from the balance between the torque and the viscous drag, is given by

$$\begin{aligned}\Omega(f) &= -F(\epsilon_2, E, \eta) \text{Im}[\tilde{b}_x \langle \cos^2 \theta \rangle + \tilde{b}_y \langle \sin^2 \theta \rangle], \\ &= -F(\epsilon_2, E, \eta) \text{Im}[\tilde{b}_x] = -F(\epsilon_2, E, \eta) \text{Im}[\tilde{b}_y] \equiv -F(\epsilon_2, E, \eta) \text{Im}[\tilde{b}_{xy}],\end{aligned}\quad (3)$$

where $\text{Im}[\dots]$ indicates taking the imaginary parts of $[\dots]$, the angular brackets denote a time average, and F is a coefficient which is proportional to the square of magnitude of field E^2 , but being inversely proportional to the dynamic viscosity η of the host medium. For spherical cells, $F = \epsilon_2 E^2 / 2\eta$. Regarding η , spin friction expression suffices for spherical particle. However, for spheroidal particles or many particles interacting in a suspension, we must consider the more complicated suspension hydrodynamics. Since the angular velocity of the rotating field is much greater than the electrorotation angular velocity, i.e., $\omega \gg \Omega$, the time averages are just equal to 1/2. For a single coated spheroidal particle, the dipole factor \tilde{b}_z is given by [10,16]

$$\tilde{b}_{xy} = \frac{1}{3} \frac{(\tilde{\epsilon}_s - \tilde{\epsilon}_2)[\tilde{\epsilon}_s + L_{xy}(\tilde{\epsilon}_1 - \tilde{\epsilon}_s)] + (\tilde{\epsilon}_1 - \tilde{\epsilon}_s)y[\tilde{\epsilon}_s + L_{xy}(\tilde{\epsilon}_2 - \tilde{\epsilon}_s)]}{(\tilde{\epsilon}_s - \tilde{\epsilon}_1)(\tilde{\epsilon}_2 - \tilde{\epsilon}_s)yL_{xy}(1 - L_{xy}) + [\tilde{\epsilon}_s + (\tilde{\epsilon}_1 - \tilde{\epsilon}_s)L_{xy}][\tilde{\epsilon}_2 + (\tilde{\epsilon}_s - \tilde{\epsilon}_2)L_{xy}]} \quad (4)$$

where y is the volume ratio of the core to the whole coated spheroid.

We are now in a position to represent b_{xy} in the spectral representation. In what follows, we will show that from the spectral representation, we can obtain the analytic expression for the characteristic frequency at which the maximum ER velocity occurs. Let $\tilde{\epsilon}_1 = \tilde{\epsilon}_2(1 - 1/\tilde{s})$, and assume $x = \tilde{\epsilon}_s/\tilde{\epsilon}_2$, we obtain

$$\tilde{b}_{xy} = NP + \frac{F_1}{\tilde{s} - s_1} \quad (5)$$

where NP denotes the nonresonant part [12] which vanishes in the limit of unshelled spheroidal cells. In Eq.(5), the various quantities are given by

$$\begin{aligned} s_1 &= \frac{L_{xy}\{1 - (1 - x)[1 - (1 - L_{xy})(1 - y)]\}}{x + (1 - L_{xy})L_{xy}(1 - x)^2(1 - y)}, \\ F_1 &= \frac{-x^2y}{3[x + (1 - L_{xy})L_{xy}(1 - x)^2(1 - y)]^2}, \\ NP &= \frac{[L_{xy}(1 - x) + x](1 - x)(1 - y)}{3[-x - (1 - L_{xy})L_{xy}(1 - x)^2(1 - y)]}. \end{aligned}$$

Note that we have assumed x to be a real number, that is, $x \approx \sigma_s/\sigma_2$, which will be justified below. After substituting $\tilde{\epsilon} = \epsilon + \sigma/i2\pi f$ into Eq.(5), we rewrite \tilde{b}_{xy} after simple manipulations

$$\tilde{b}_{xy} = (NP + \frac{F_1}{s - s_1}) + \frac{\delta\epsilon}{1 + if/f_c} \quad (6)$$

with $s = (1 - \epsilon_1/\epsilon_2)^{-1}$ and $t = (1 - \sigma_1/\sigma_2)^{-1}$, where the dispersion magnitude and characteristic frequency admit respectively

$$\delta\epsilon = F_1 \frac{s - t}{(t - s_1)(s - s_1)}, \quad (7)$$

$$f_c = \frac{1}{2\pi} \frac{\sigma_2}{\epsilon_2} \frac{s(t - s_1)}{t(s - s_1)}. \quad (8)$$

III. NUMERICAL RESULT

In Fig.1(a)-(c), the dependence of the pole, characteristic frequency and dispersion magnitude on the parameter x are investigated for different particle shape. For clarity, we set

$z = 1/y$ from now on. It is evident that both s_1 and f_c decreases monotonically as x increases; larger depolarization factor leads to smaller s_1 and f_c . However, for increasing x , $\delta\epsilon$ increases concomitantly; also, $\delta\epsilon$ increases while L_z increases.

In Fig.1(d)-(f), we investigate the dependence of the pole, characteristic frequency and dispersion magnitude on x for different shell thickness. For $z = 1$, namely without shell, $s_1 = 0.3(= L_{xy})$ always. Increasing x leads to decreasing s_1 or f_c . It is evident that thicker shell yields larger pole or f_c as $x < 1$, but smaller as $x > 1$. In the dispersion magnitude plot, $\delta\epsilon$ is constant for the uncoated particles. In the case of coated particles, increasing x yields increasing $\delta\epsilon$; moreover, larger z , smaller $\delta\epsilon$.

In Fig.2, the dependence of material parameters (namely, s , t , ϵ_2 , and σ_2) on f_c and $\delta\epsilon$ is discussed. f_c is weakly dependent on s , but strongly dependent on t , ϵ_2 and σ_2 . Smaller $|t|$ (or ϵ_2), larger f_c . However, larger σ_2 , larger f_c . On the other hand, $\delta\epsilon$ is weakly dependent on s and t . Also, it is evident that ϵ_2 and σ_2 play no role in $\delta\epsilon$, as Eq.(7) actually shows. Note all curves in Fig.2(g) and (h) are respectively overlapped. In other words, this predicts that ϵ_2 and σ_2 plays no role in the peak value of the angular velocity (see Fig.4).

In Fig.3, the dependence of L_z , z and x on $-Im[b_{xy}]$ are investigated, respectively. There is always a peak, the location of which is just the characteristic frequency f_c . As L_z (or x) increases, f_c becomes red-shift, while the corresponding peak value increases as well. However, a larger z yields smaller peak value, while f_c is changed weakly.

In Fig.4, we discuss the dependence of s , t , ϵ_2 and σ_2 on $-Im[b_{xy}]$. The s effect is small so that it can be neglected. Smaller $|t|$ leads to larger f_c ; at the same time, increasing peak value appears. Increasing ϵ_2 yields decreasing f_c , and the related peak value is unchanged. For increasing σ_2 , f_c increases concomitantly, but the peak value remains unchanged as well.

In Fig.5, the experimental data is extracted from an experiment on human erythrocytes [14]. Obviously, there is a good agreement between theory and experiment. During this fitting, we model the cell as oblate spheroid ($L_z = 0.65$).

IV. DISCUSSION AND CONCLUSION

In the present work, we have discussed the effect of oblate spheroidal particle shape on the ER spectrum. In reality, there exist many cells in the form of oblate spheroid, such as human erythrocytes [9]. However, there exist only a few theories to discuss the ER spectrum of such cells (e.g., [14] and references therein). Our theory is advantageous in that the characteristic frequency at which the maximum rotational velocity occurs, is derived analytically, which simplifies the fitting of experimental data.

We have assumed x , namely the ratio of the shell to host dielectric constant, to be a real and positive number. In fact, its imaginary part is indeed small. If we had retained the imaginary part of x , two peaks would appear, and the conductivity-dominated peak would have occurred at substantially lower frequency. Therefore, the neglect of the imaginary part of x is to drop the lower frequency peak. Moreover, according to our calculations, there are two (degenerate) sub-dominant poles associated with b_{xy} in the spectral representation. Thus, in the present work, only one capacitance-dominated peak has been shown.

In a recent work [10], we developed simple equations to describe the ER of particles in a suspension from the spectral representation, and obtained a good fitting on a coated-bead ER assay by using the coated spherical model. In this work, an extension to oblate spheroidal case has been made. Our theory serves as a basis which describes the parameter dependence of the polarization and thereby enhances the applicability of various cell models for the analysis of the polarization mechanisms. In this connection, the shell-spheroidal cell model may readily be extended to multi-shell cell model. However, we have shown that the multi-shell nature of the cell may have a minor effect on the ER spectrum [17].

We have considered the isolated cell case, which is a valid assumption for low concentration of cells. However, for a higher concentration of cells, we should consider the mutual interaction between cells. When the volume fraction of the suspension becomes large, the particles may aggregate in the plane of the rotating applied field, and the mutual interactions between the suspended particles can modify the spin friction, which is a key to determine

the angular velocity of ER. For ER of two particles, we have successfully applied the spectral representation to deal with the dispersion frequency [7]. However, the determination of the spin friction is still lacking. For two particles, the basic tool is the reflection method [18], being analogous to the multiple image method in electrostatics, but being only valid for two particles. For more than two particles, we need a first-principles method, e.g., the Green's function (Oseen tensor) formulation. For a dilute suspension, however, one may adopt the effective medium theories [19] to capture the effective viscosity of a suspension, hence modifying further the ER spectrum.

One may argue that normal erythrocytes may deviate from an oblate spheroidal shape. For cells of non-conventional shapes, one may use a first-principles approach [20], recently developed to deal with particles of rod shape. As shown in Ref. [20], the derivation from spheroidal model can be small when the cells are rotating with their long axes along the applied field.

In summary, we have presented a theoretical study of electrorotation based on the spectral representation theory. From the theoretical analysis, we find that cell shape as well as the coating can change the characteristic frequency. By adjusting the cell shape, dielectric properties and the thickness of the coating, it is possible to obtain good agreement between our theoretical predictions and the experimental data on human erythrocytes suspensions.

ACKNOWLEDGMENTS

This work was supported by the Research Grants Council of the Hong Kong SAR Government under grant CUHK 4245/01P. K.W.Y. acknowledges useful conversation with Professor G. Q. Gu.

REFERENCES

- [1] For a review, see J. Gimsa and D. Wachner, *Biophys. J.* **77**, 1316 (1999).
- [2] J. Gimsa, *Ann. NY Acad. Sci.* **873**, 287 (1999).
- [3] K. Asami, T. Hanai and N. Koizumi, *Jpn. J. Appl. Phys.* **19**, 359 (1980).
- [4] G. Fuhr, J. Gimsa and R. Glaser, *Stud. Biophys.* **108**, 149 (1985).
- [5] J. Gimsa, P. Marszalek, U. Lowe and T. Y. Tsong, *Biophys. J.* **73**, 3309 (1991).
- [6] G. De Gasperis, X.-B. Wang, J. Yang, F. F. Becker and P. R. C. Gascoyne, *Meas. Sci. Technol.* **9**, 518 (1998).
- [7] J. P. Huang, K. W. Yu and G. Q. Gu, *Phys. Rev. E* **65**, 021401 (2002).
- [8] K. W. Yu and Jones T. K. Wan, *Comput. Phys. Commun.* **129**, 177 (2000).
- [9] K. Asami and T. Yamaguchi, *Annals of Biomedical Engineering* **27**, 427 (1999).
- [10] J. P. Huang and K. W. Yu, *J. Phys.: Condens. Matter* **14**, 1213 (2002).
- [11] D. J. Bergman, *Phys. Rep.* **43**, 379 (1978).
- [12] K. P. Yuen and K. W. Yu, *J. Phys.: Condens. Matter* **9**, 4669 (1997).
- [13] Jun Lei, Jones T. K. Wan, K. W. Yu and Hong Sun, *Phys. Rev. E* **64**, 012903 (2001).
- [14] J. Gimsa, Th. Schnelle, G. Zechel, and R. Glaser, *Biophys. J.* **66**, 1244 (1994).
- [15] J. Gimsa, *Bioelectrochemistry* **54**, 23 (2001).
- [16] L. Gao, Jones T. K. Wan, K. W. Yu and Z. Y. Li, *J. Phys.: Condens. Matter* **12**, 6825 (2000).
- [17] J. P. Huang, K. W. Yu, J. Lei and H. Sun, *Commun. Theor. Phys.*, in press (2002).
- [18] J. Happel and H. Brenner, *Low Reynolds number hydrodynamics*, (Kluwer Academic Publishers, Dordrecht/Boston/London, 1983).

[19] T. C. Choy, *Physica A* **221**, 263 (1995).

[20] Jun Lei, Jones T. K. Wan, K. W. Yu and Hong Sun, *J. Phys.: Condens. Matter* **13**, 3583 (2001).

FIGURES

FIG. 1. FIG.1. The dependences of pole, characteristic frequency and dispersion magnitude on x for $s = 1.1$, $t = -0.005$, $\epsilon_2 = 80\epsilon_0$, $\sigma_2 = 2.9 \times 10^{-5}S/m$. (a)~(c) $z = 2$; (d)~(f) $L_z = 0.4$.

FIG. 2. FIG.2. The dependence of characteristic frequency and dispersion magnitude on x for $z = 6$, $L_z = 0.4$. (a) $t = -0.005$, $\epsilon_2 = 80\epsilon_0$, $\sigma_2 = 2.9 \times 10^{-5}S/m$; (b) $s = 1.1$, $\epsilon_2 = 80\epsilon_0$, $\sigma_2 = 2.9 \times 10^{-5}S/m$; (c) $t = -0.005$, $s = 1.1$, $\sigma_2 = 2.9 \times 10^{-5}S/m$; (d) $s = 1.1$, $t = -0.005$, $\epsilon_2 = 80\epsilon_0$; (e) $t = -0.005$, $\epsilon_2 = 80\epsilon_0$, $\sigma_2 = 2.9 \times 10^{-5}S/m$; (f) $s = 1.1$, $\epsilon_2 = 80\epsilon_0$, $\sigma_2 = 2.9 \times 10^{-5}S/m$; (g) $t = -0.005$, $s = 1.1$, $\sigma_2 = 2.9 \times 10^{-5}S/m$; (h) $t = -0.005$, $s = 1.1$, $\epsilon_2 = 80\epsilon_0$.

FIG. 3. FIG.3. The dependence of $-Im[b_{xy}]$ on frequency for $s = 1.1$, $t = -0.005$. (a) $\epsilon_2 = 80\epsilon_0$, $\sigma_2 = 2.9 \times 10^{-5}S/m$, $z = 6$, $x = 2$; (b) $\epsilon_2 = 80\epsilon_0$, $\sigma_2 = 2.9 \times 10^{-5}S/m$, $L_z = 0.4$, $x = 2$; (c) $\epsilon_2 = 80\epsilon_0$, $\sigma_2 = 2.9 \times 10^{-5}S/m$, $z = 6$, $L_z = 0.4$.

FIG. 4. FIG.4. The dependence of $-Im[b_{xy}]$ on frequency for $x = 2$, $z = 6$, $L_z = 0.4$; (a) $t = -0.005$, $\epsilon_2 = 80\epsilon_0$, $\sigma_2 = 2.9 \times 10^{-5}S/m$; (b) $s = 1.1$, $\epsilon_2 = 80\epsilon_0$, $\sigma_2 = 2.9 \times 10^{-5}S/m$; (c) $t = -0.005$, $s = 1.1$, $\sigma_2 = 2.9 \times 10^{-5}S/m$; (d) $t = -0.005$, $s = 1.1$, $\epsilon_2 = 80\epsilon_0$.

FIG. 5. FIG.5. A fitting on human erythrocyte data. Experiment: $\sigma_2 = 12.5 \times 10^{-3}$. Theory: $s = 100$, $t = 1.00783$, $\epsilon_2 = 80\epsilon_0$, $z = 3$, $x = 0.008$, $L_z = 0.65$, $F/E^2 = 135$.

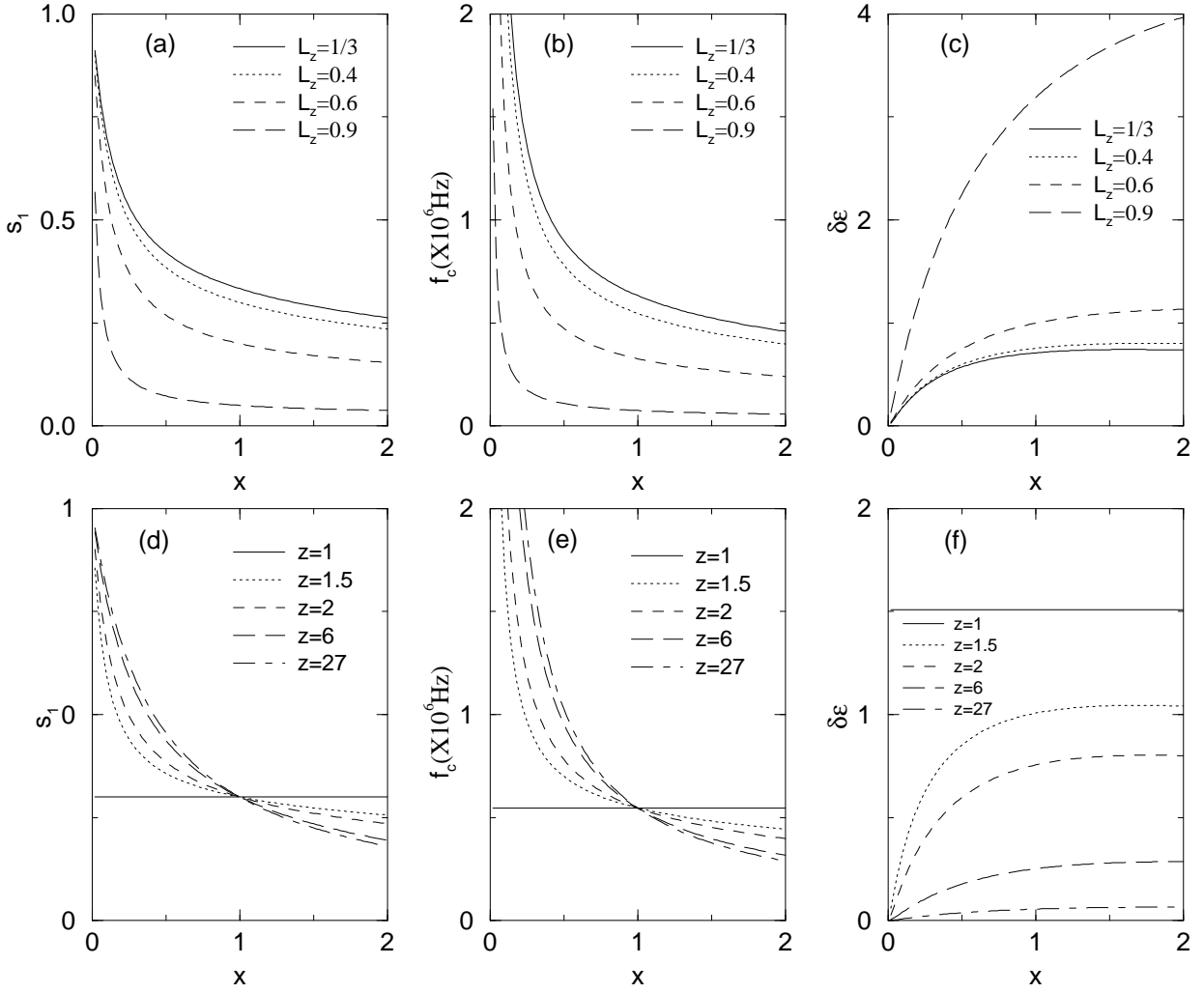


FIG.1

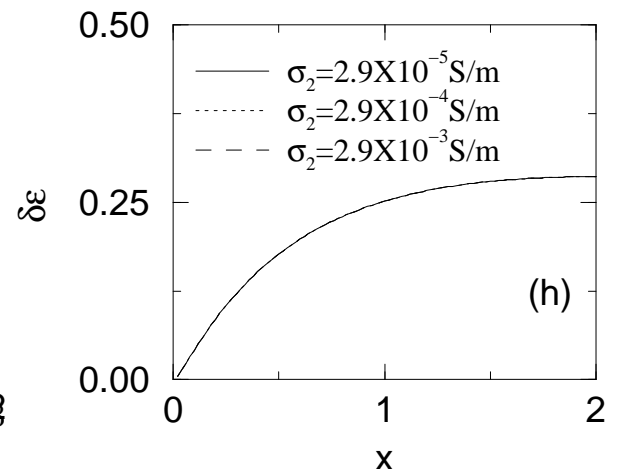
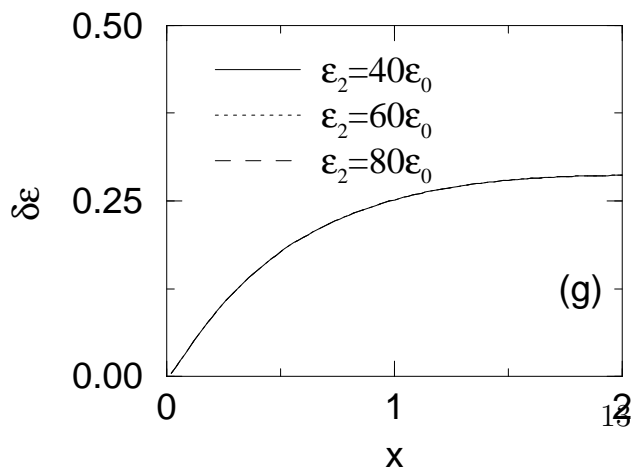
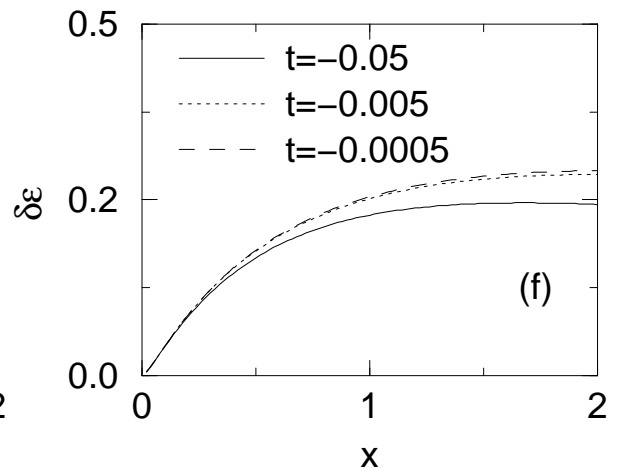
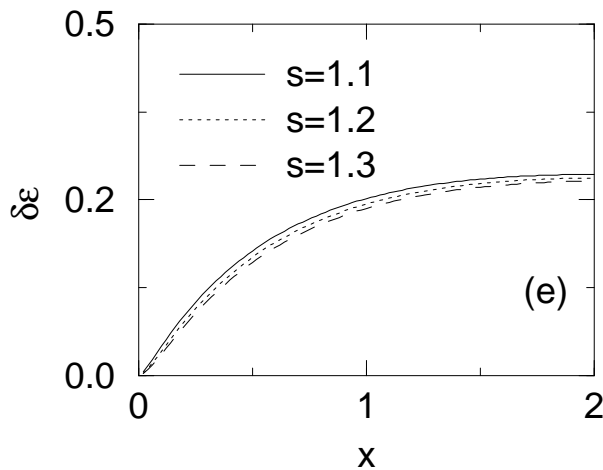
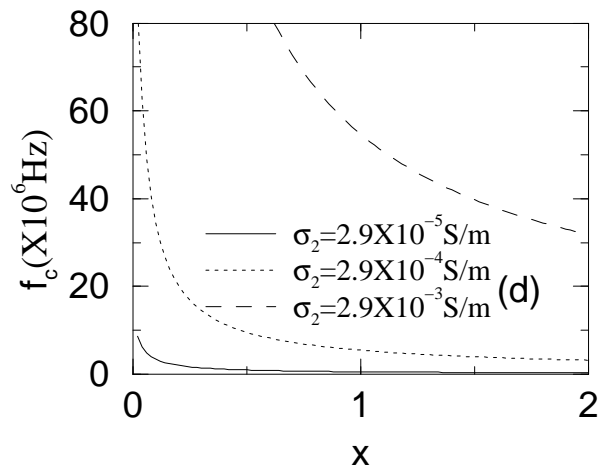
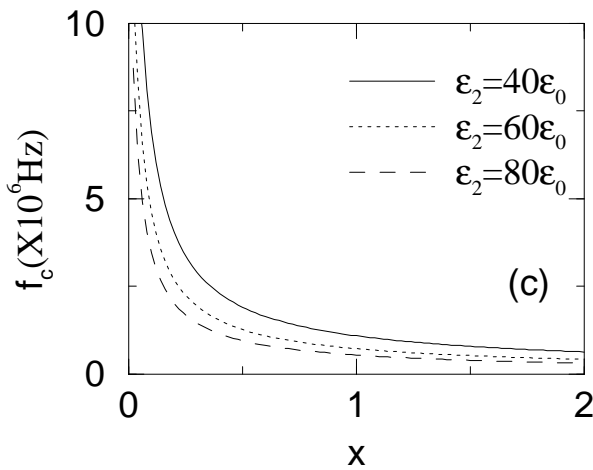
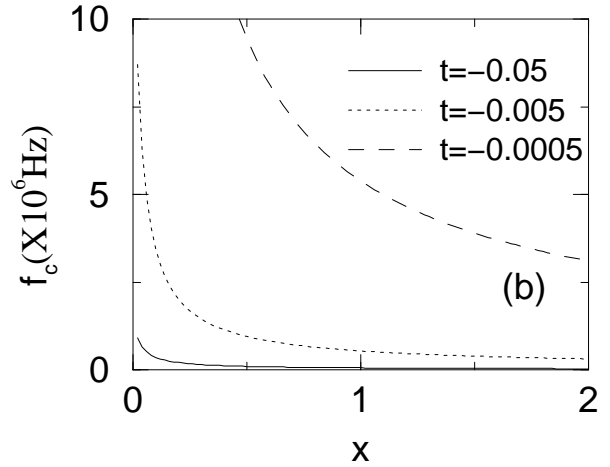
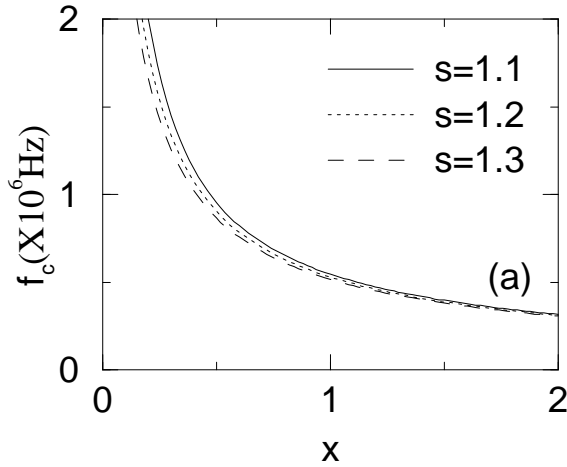


FIG.2

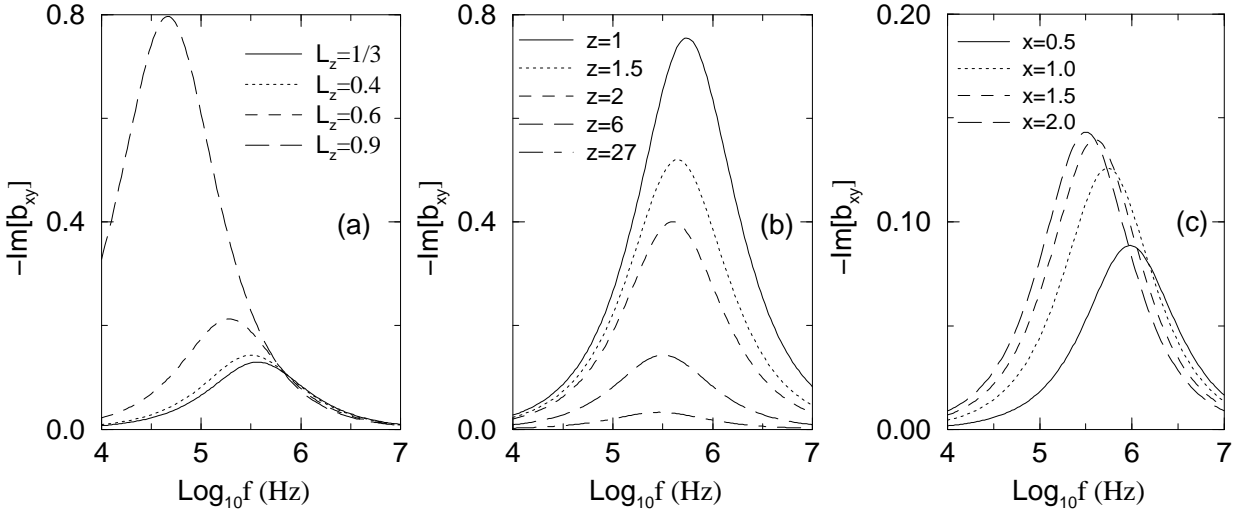


FIG.3

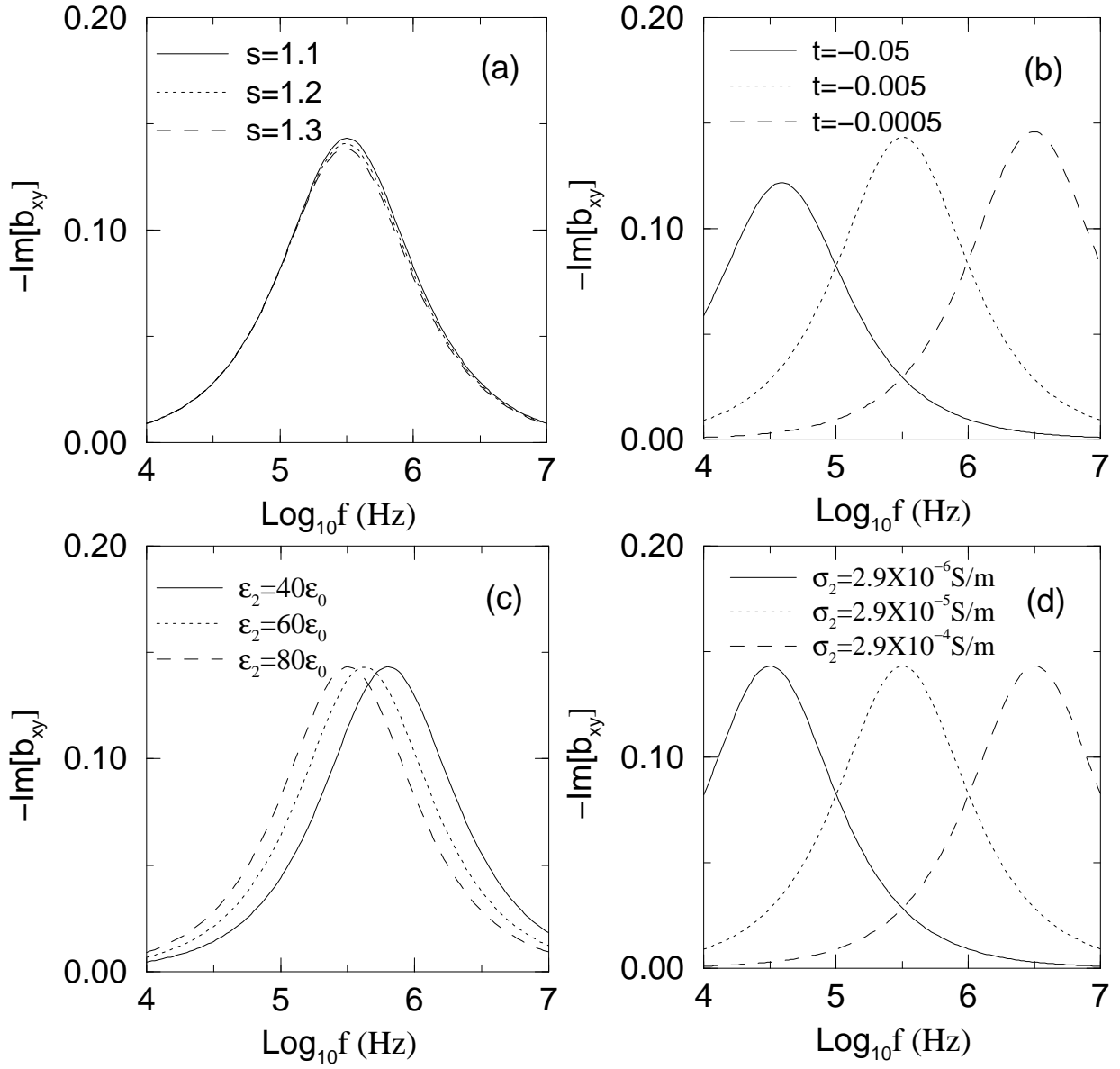


FIG.4

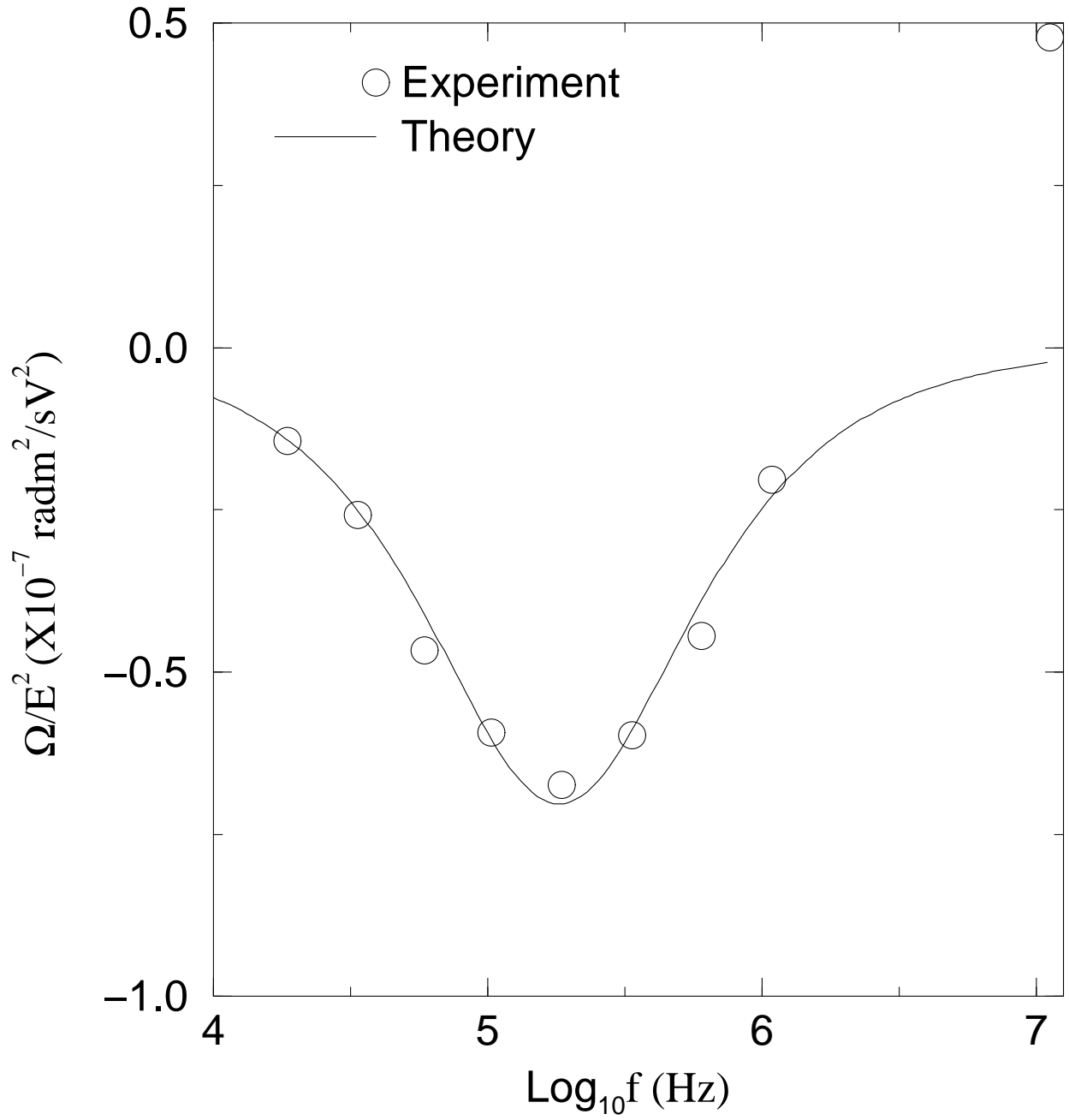


FIG.5